Tool life and hole surface integrity studies for hole-making of Ti6Al4V Alloy

Zhao, Q., Qin, X., Ji, C., Li, Y., Sun, D., & Jin, Y. (2015). Tool life and hole surface integrity studies for hole-making of Ti6Al4V Alloy. *International Journal of Advanced Manufacturing Technology*, *79*(5-8), 1017-1026. https://doi.org/10.1007/s00170-015-6890-z

Published in:
International Journal of Advanced Manufacturing Technology

Document Version:
Peer reviewed version

Queen's University Belfast - Research Portal:
Link to publication record in Queen's University Belfast Research Portal

Tool Life and Hole Surface Integrity Studies for Hole-making of Ti6Al4V Alloy

Xuda Qin, Qing Zhao, Chunhui Ji, Yonghang Li, Dan Sun, Yan Jin

Abstract: With a significant growth in use of titanium alloys in aviation manufacturing industry, the key challenge of making high quality holes in aircraft assembly process needs to be addressed. In this work, case studies deploying traditional drilling and helical milling technologies are carried out to investigate the tool life and hole surface integrity for hole-making of titanium alloy. Results show that , the helical milling process leads to much longer tool life, lower cutting force, generally lower hole surface roughness and higher hole subsurface microhardness. In addition, no plastically deformed layer or white layer have been observed in holes produced by helical milling. In contrast, a slightly softened region was always present on the drilled surface. The residual stress distributions within the hole surface, including compressive and tensile residual stress, have also been investigated in detail.

***Keywords*:** Titanium Alloy; Surface integrity; Drilling; Helical milling

1. Introduction

Titanium alloys have been widely used in the aerospace and automotive industries due to their superior mechanical properties, corrosion resistance and heat resistance. The alloys also find widespread applications in surgical, chemical and ship building.

However, titanium alloys have very poor machinability, this may be because they are highly reactive and may lead to cold welding during the machining process, which in turn causes chipping and premature tool failure [1]. In addition, its low thermal conductivity would lead to rapid temperature rise at the tool/workpiece interface, hence reduces the tool life. In addition, the high strength and modulus of elasticity of the alloy at elevated temperature could further impair its machinability [2].

To date, numerous research efforts have been focused on the turning and milling operations of Ti6Al4V [3-8]. Many experimental studies focused on the tool wear mechanisms of binderless cubic boron nitride (BCBN) tool in high-speed milling process for Ti6Al4V. At the same time, natural diamond tools have proven their excellent cutting performance in machining of titanium. In addition, the quality of surface machined with the natural diamond tool was found to be better than those machined with other cutting tools. However, the above studies are not applicable to hole-making process due to the different nature of operations.

Hole-making process accounts for 40–60% of total material removal processes in aircraft assembly and therefore is considered a key process in aerospace industries [9]. Drilling is a traditional hole-making technique and is usually among the final steps in fabrication of mechanical components, therefore it is considered to have more economical impact [1]. Sharif et al. [10] carried out drilling performance and tool life studies of carbide tools with different coatings (TiAlN and supernitride) in drilling of Ti-6Al-4V. They confirmed that the higher percentage of aluminum content in the supernitride coating recorded the lowest tool wear rate. Zeilmann et al. [11] studied the cutting temperature in drilling of Ti6Al4V using minimal quantity of lubricant (MQL) technology, and found that the cutting temperature with application of MQL internally through the tool has been reduced by 50 % as compared to those with MQL applied with an external nozzle. Cantero et al. [12] also studied

the drilling process of Ti6Al4V under dry cutting conditions at cutting speeds ranged from 25 to 65 m/min; they suggested that moderate cutting parameters need to be employed to prolong the tool life.

Surface integrity is an important aspect to consider when evaluating the quality of a machined surface. Several studies on the machined surface integrity have been carried out, and a white layer was usually observed under dry conditions [13-15]. In dry drilling of Ti-6Al-4V, the machined surface showed 30% increase in microhardness in the top 75 μm thick layer as compared to the original alloy surface when the tool failed. In addition, the thickness of the affected zone increases with the drilling time [12]. Erween et al. [16] proved that the surface roughness can be greatly improved by increasing cutting speeds in drilling of Ti-6Al-4V and Ti-5Al-4V-Mo/Fe, the cutting speed and the tool wear were found to be important factors affecting the metallurgical alteration and the microhardness of machined surfaces for both alloys.

Recently, helical milling has been regarded as an innovative method with a number of advantages: the intermittent cutting process, smaller thrust force, and the higher accuracy compared with the conventional drilling. Iyer et al. [17] proved that the helical milling is capable of machining H7 quality holes with a surface finish of 0.3 μm in AISI D2 tool steel. Hiroyuki et al. [18] compared the drilling and helical milling process of aluminum alloy, it is found that the cutting temperature, shape error and the burr formation in the helical feed milling with MQL, are all reduced when compared with the drilling process. Brinksmeier et al. [19] established a helical milling kinematics model, which described mathematically the occurring conditions through considering the engagement angle as the function of the following parameters: hole diameter, tool diameter and gradient of the helical course. Based on the improved Z-map model, a 3D surface topography model was also developed to simulate the surface finish profile in helical milling processes [20]. Liu et al. [21] proposed an analytical model dealing with time domain cutting force, which is a function of helical feed, spindle velocity, axial and radial cutting depth, as well as milling tool geometry. Denkena et al. [23] investigated the influence of the axial and tangential feed on cutting forces and borehole quality during helical milling of layer compounds consisting of unidirectional carbon fiber reinforced plastic (CFRP) and Ti-6Al-4V. Helical milling technology has also demostrated significant enhancement in the resulting hole quality compared to conventional drilling in composite machining, due to the reduced axial force and cutting temperature [22]. However, reports on the performance of helical milling operations for titanium alloys are still lacking.

The detailed helical milling kinematics is shown in Fig.1. There are three motions in helical milling process, namely, orbital rotation, spindle rotation and axial feed. There are three main cutting parameters namely: n: spindle rotation speed (rpm), S_t: tangential feed (mm/tooth), and a: axial feed (mm).

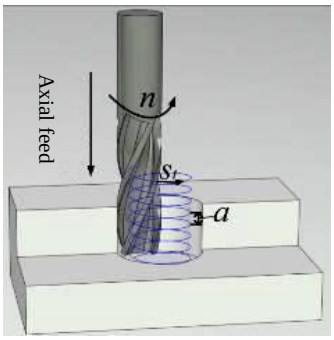

Fig.1 Helical milling kinematics

The machined surface integrity is generally defined by three parameters [24].

(1) A geometric parameter: Roughness

(2) A mechanical parameter: Residual stresses

(3) A metallurgical parameter: Microstructure and microhardness

In this work, the hole-making processes were studied for titanium alloy using traditional drilling and helical milling. The evolution the surface integrity deploying new or worn tools has been investigated during hole-making operations. The effects of tool wear on the axial force and surface integrity of the holes are also elucidated.

2. Experimental Set-up

2.1 Workpiece materials and cutting tools

The titanium alloy (Ti-6Al-4V) workpiece (250 mm ×120 mm ×10 mm) was supplied by BAOJI TITANIUM INDUSTRY CO., LTD. The nominal chemical compositions of the alloy (in wt. %) are given in Table 1, and the mechanical properties are shown in Table 2.

Table 1 Nominal chemical compositions of Ti-6Al-4V (in wt. %)

Element	Ti	Al	V	Fe	Si	C	N	H	O
Wt. %	base	5.5-6.8	3.5-4.5	≤0.3	≤0.1	≤0.1	≤0.05	≤0.015	≤0.015

Table 2 Mechanical properties of Ti-6Al-4V

Item	Elongation (%)	Thermal conductivity (W/m·℃)	Modulus of elasticity (GPa)	Tensile strength (MPa)	Hardness (HV)
Value	13	8.37	115	932	330

Straight tungsten carbide coated tools were used for the drilling tests. The inserts were manufactured by Sandvik Coromant (reference R846-1000-30-A1A 1220). Drilling tests were conducted under the conditions as detailed in Table 3.

Tools with ultra-fine grain carbide coated inserts were specifically designed for the helical milling tests in this work. The composition of the cutter matrix is WC-8% Co, and the thickness of the TiAlN coating is 1-3 μm. Helical milling tests were conducted under the conditions as shown in Table 4.

Table 3 Cutting conditions for drilling tests

Tool geometries	Diameter: 10 mm, helix angle: 37.589° point angle: 140°, Number of teeth: 2

Cutting speed	66 m/min
Feed	0.2 mm/rev
Cooling condition	Dry
Hole diameter	10 mm
Hole depth	10 mm

Table 4 Cutting conditions for helical milling tests

Tool geometries	Diameter: 6 mm, helix angle: 35°, rake angle: 5°, Number of teeth: 4
Cutting speed	66 m/min
Tangential feed	0.04 mm/tooth
Axial feed	0.2 mm/rev
Cooling condition	Dry
Hole diameter	10 mm
Hole depth	10 mm

2.2 Machining tests

The experiments were performed on a five-axis machining center DMC75Vlinear with a maximum spindle speed of 28,000 rpm (See Fig.2). The Kistler three-direction stationary dynamometer (Model: 9257A) was placed under the workpiece, and the supporting Kistler charge amplifier (Type: 5070) was attached to obtain the three-direction cutting forces (marked as F_x, F_y, F_z, respectively).

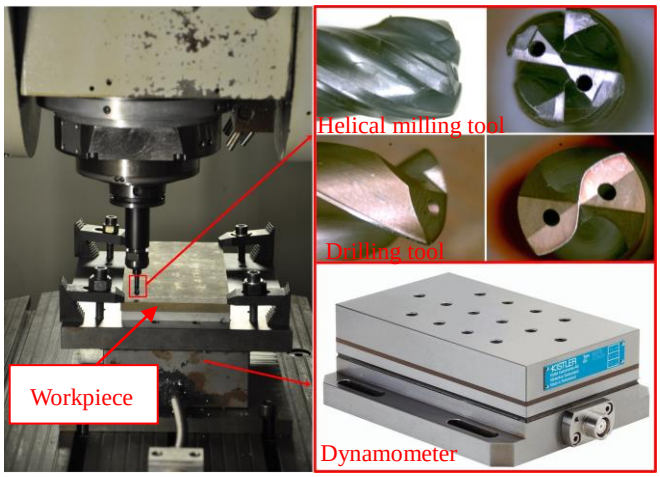

Fig.2 Experimental setup and cutting forces measurement

Tool wear was examined using an optical microscope, the photos of the tool flank wear were taken by a SI-DUSB-8-1300k digital camera. Further tool wear analysis was conducted using Quanta FEG250 scanning electron microscope (SEM). The failure or rejection of a tool is often based on the following criteria [25]:

(1) When the average non-uniform flank wear VB reached 0.2 mm;

(2) When the maximum flank wear VB_{max} reached 0.3 mm;

(3) Excessive chipping/flaking or catastrophic failure.

Surface roughness values of the machined holes were measured using Mitutoyo SJ-500 with a cut-off length of 0.8 mm, and the measurements were performed three times for each hole to obtain the average surface roughness.

To understand the evolution of the metallurgical properties of the worn titanium surface layer, the machined holes were sectioned in both axial and hoop directions using wire electro-discharge machining (EDM) [26]. The sectioned samples were further hot mounted in Bakelite, ground and polished using Struers Tegramin-25 polishing system before cross-sectional microstructual analysis of the machined surface. Microhardness measurements were conducted using a MHV 2000 digital microhardness tester with a load of 100 g and a dwell time of 10 s. The results of the hardness measurements are very sensitive to the local microstructure due to the different hardness of α and β phases. Optical microscopy and SEM were also applied to reveal the surface anomalies (e.g. elongated grains) generally produced by the machining operations. Furthermore, the residual stresses have been measured by X-Ray diffraction using a PROTOiXRDCOMBO diffract meter. The use of larger diameter collimator and the Psi (ψ) swing and Phi (φ) swing method would help optimizing the peak shape, and peak fitting method is used to accurately determine the peak features. Young's modulus (120.2 GPa) and Poisson's ratio (0.36) were utilized to characterized the {110} reflection. and other parameters are: no stress diffraction angle 137.4 °, ψ angle selection 0°, ± 18.7°, ± 27°, ± 33.8°, ± 39.9°, swing angle ψ ± 5°, swing angle φ ± 30°.

3 Experimental results and discussion

3.1 Tool life and tool wear in drilling and helical milling

The tool life was defined by the number of holes produced prior to the tool failure. The preliminary experiments show that the drill was rejected after drilling of 50 holes when fracture occurred at the outer corner of the drill (Maximum flank wear VB_{max}=0.45 mm). Erween et al. [16] also reported that the non-uniform flank wear and micro-chipping dominated the wear pattern for the drilling process. The tool failure probably caused by the combination of various wear mechanisms such as adhesion, diffusion and plastic deformation which are usually encountered during the machining of Ti-6Al-4V. Since the major cutting action takes place on the chisel point and the cutting edges of the drill, the major cutting edges worn more excessively compared with the minor cutting edge, Fig.3. In contrast, the specially designed helical milling cutter failed after 110 holes when the uniform wear exceeded the rejection level (VB=0.25 mm). As can be seen from Fig.4, the front cutting edge of the helical milling cutter encountered crater, adhesion and chipping. In addition, the flaking often occurred on the periphery cutting edge (See Fig.5).

The wear mechanisms involved in drilling and helical milling are very different. Firstly, in drilling process the cutting speed is essentially zero at the centre of the drill and the material removal around the chisel edge is primarily developed by the extrusion with the transport of material radically away from the centre. While the material removal along the major cutting edge is usually developed by shear operation as the cutting speed and the rake angle varied with distance from the drill centre. Additionally, rubbing operation often occurs due to the sliding motion of the hole surface against the drill clearance face at the drill periphery [15]. In contrast, during the helical milling process, , the rotating centre cutting end mill traverses the helical trajectory to generate the hole with diameter larger than that of the tool. On account of the secondary helical movement in addition to the primary cutting motion, the

material removal at and near the hole centre is developed by cutting operation rather than by extrusion. The periphery materials of hole are removed by the periphery cutting edges and the part of material at the bottom of hole is removed by the front cutting edges [27].

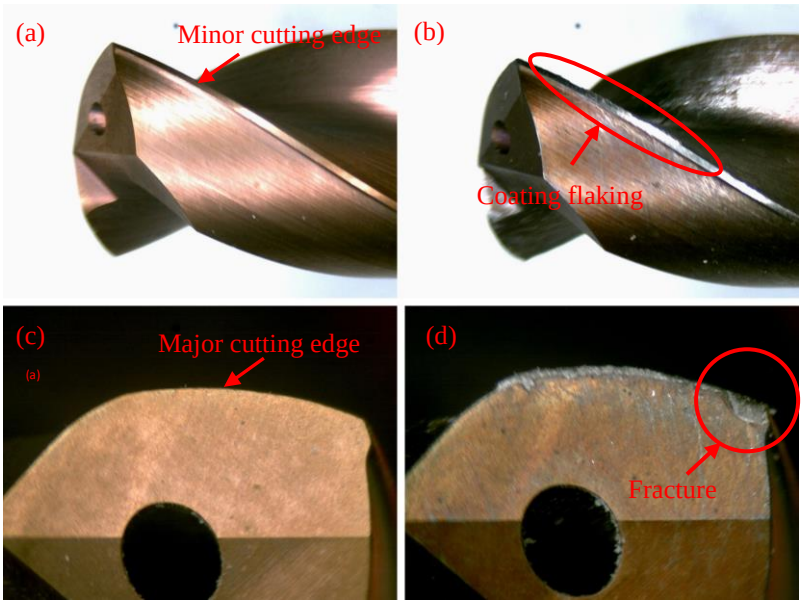

Fig.3 Optical images of drill. (a) Side view of minor cutting edge before drilling, (b) Side view of minor cutting edge after drilling, (c) Bottom view of major cutting edge before drilling and (d) Bottom view of major cutting edge after drilling.

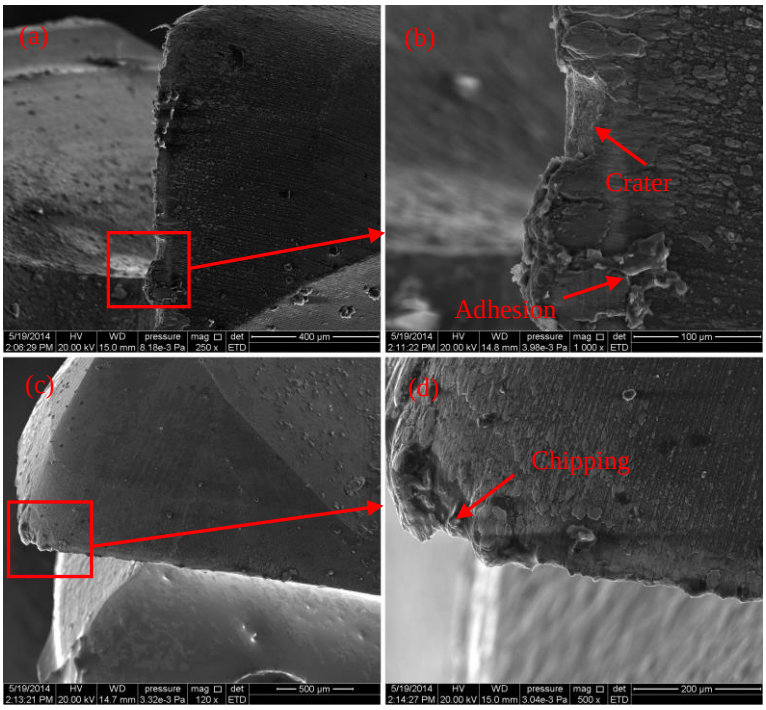

Fig.4 SEM images of the front cutting edge of a failed helical milling cutter

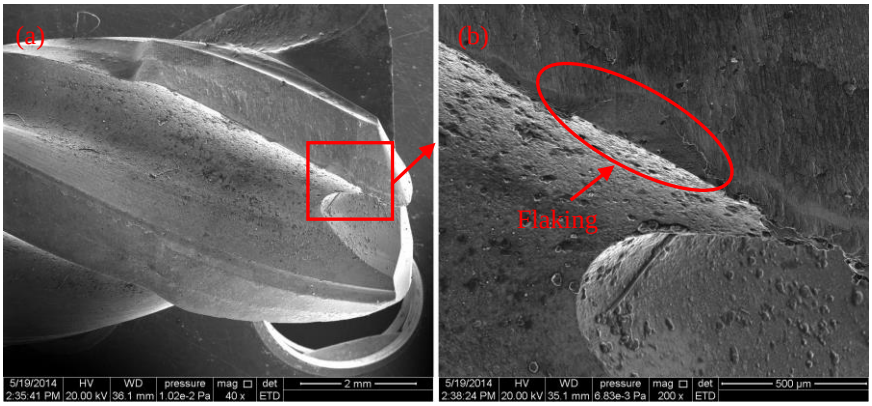

Fig.5 SEM images of the periphery edge of a failed helical milling cutter

3.2 Cutting force in drilling and helical milling

The cutting forces for drilling and helical milling processes have been plotted in Figs. 6 and 7, respectively. For the drilling process (Fig. 6), the cutting force gradually increases with hole number, this is largely due to the gradually increase in tool wear, chipping or even tool surface fracture. The radial force (F_x/F_y) is much lower than the axial force (F_z), and remains stable during the whole drilling process, corresponding to a slower wear process of the minor cutting edge. However the radial force produced in helical milling process gradually increases with increasing hole number (See Fig.7). This is because the the minor cutting edge only plays the supporting cutting role in the drilling process, while the periphery edge of helical milling cutter plays the dominant role for the formation of the hole wall [22].

By comparing the cutting force generated during drilling and helical milling processes under the same cutting conditions (Figs 6(b) and 7 (b)), it can be found that the maximum thrust force of helical milling is much lower than that of drilling process. The maximum axial force is about 250 N in helical milling and about 1700 N in drilling process. The higher axial force in drilling is the result of material extrusion associated with the highly negative rake angles and zero cutting speed at the drill centre. The material removal regime in this region is mainly by a process resembling extrusion rather than cutting motion.

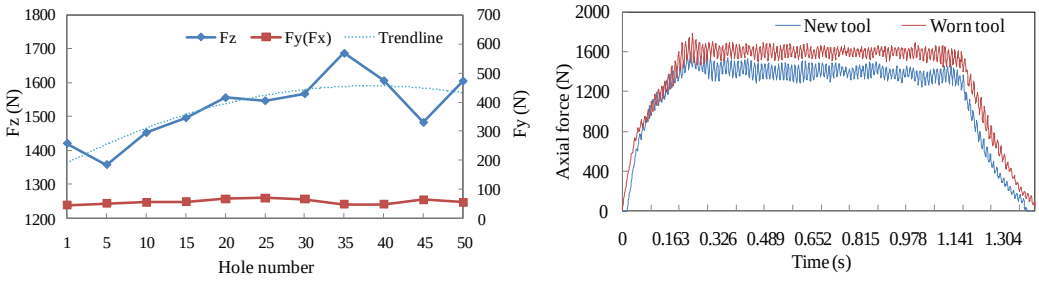

(a) (b)

Fig. 6 Drilling process. (a) Cutting force vs. hole number, and (b) Cutting force of one hole for new and worn drills

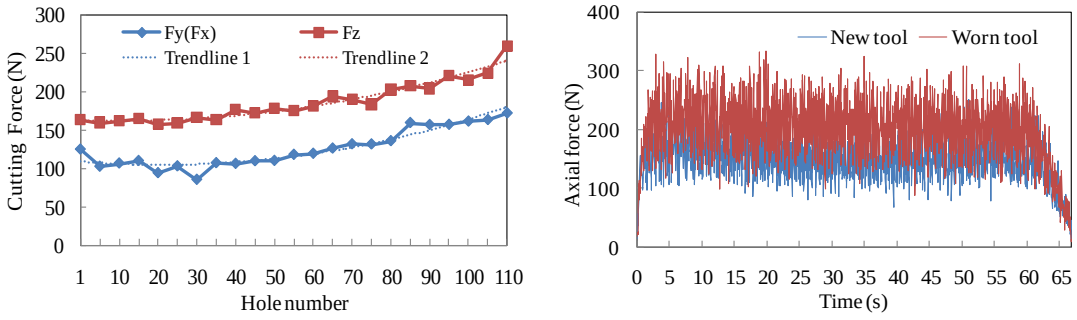

(a) (b)

Fig. 7 Helical milling process. (a) Cutting force vs. hole number, and (b) Cutting force of one hole for new and worn tool

3.3 Hole surface integrity in drilling and helical milling

3.3.1 Surface roughness

Fig.8 shows the average hole surface roughness values generated for helical milling and drilling processes. It can be seen that the surface roughness ranges from 0.67 to 1.06 μm for drilling and from 0.71 to 2.69 μm for helical milling process. In the initial stage, the surface roughness for drilling and helical milling shows similar trend. Slightly higher surface roughness values have been recorded in helical milling at the intermediate stage compared to the drilling process. As the helical milling cutter worn further, the roughness significantly increased and the maximum value reached 2.69 μm. However, the roughness value in drilling process gradually decreases with increasing tool wear, and the surface finish tends to be smoother toward the failure point. This is probably due to the considerable smearing of the workpiece surface when the worn tool was used [15]. However, the surface roughness increases significantly when the tool approaches failure in helical milling, this is mainly because in helical milling process the front cutting edge and the periphery cutting edge both contribute to the materials removal process, as explained earlier. As the cutting tool descends during helical milling, the surface of periphery edge gradually deteriorates, which leads to an increase in the hole surface roughness. Additionally, materials transferred to the cutting tool may also result in rapid increase of hole surface roughness. Therefore, the periphery edge of the cutting tool in helical milling plays a key role in determining the hole surface condition.

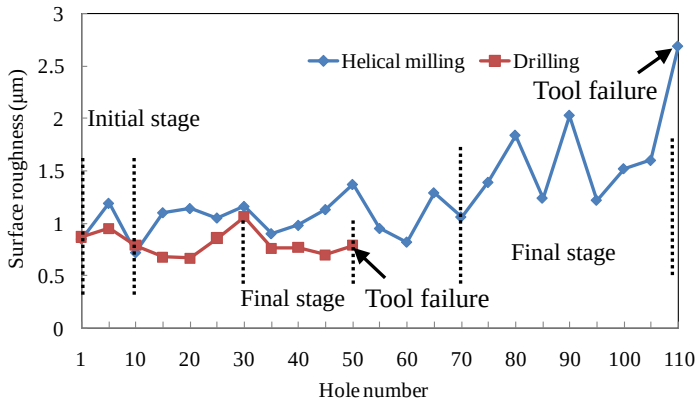

Fig.8 Surface roughness measurements in drilling and helical milling processes.

3.3.2 Subsurface microhardness characterization

The measurement of subsurface microhardness was performed every 20 μm down to 180 μm underneath the machined surface for the drilled workpiece, and down to 200 μm for the workpiece processed by helical milling. The average results for each depth have been plotted, as shown in Fig.9. It should be noted that for drilling process, the results obtained from different stages of tool life show similar trend. More specifically, the microhardness at 20 μm underneath the machined surface is lower than that of bulk material (330 HV). The slight drop at the initial stage (first 20 μm underneath the machined surface) is often attributed to the thermal softening. The microhardness of subsurface material rises slightly to 350-375 HV before it drops to bulk hardness value at 100 μm underneath the surface and stabilizes at that level. Moreover, the minimum microhardness value is about 7% lower than the bulk material hardness, and the maximum microhardness value in drilling is both 10% higher than the bulk material hardness, this is mainly due to the slightly minor cutting edge wear. As is shown in Fig.9 (b), softened surface layer did not appear for helical milling process, and the maximum cutting temperature is about 200℃[28] due to the eccentric machining process and good heat dissipation. The resulting cutting temperature in helical milling is much lower than the phase transformation temperature of Ti-6Al-4V (985℃). It should also be noted that the maximum microhardness value in helical milling was approximately 18% higher than that of the bulk material, this is mainly caused by the greater input of mechanical energy. Also the tool wear is responsible for the change of the alloy microstructure and the hardness values usually increase with increasing tool wear.

When the workpiece material is subjected to a high cutting temperature and high cutting pressure under dry machining, a competing process between work hardening and thermal softening takes place and affects the fundamental behaviors of the workpiece material. For the microhardness measurements depicted in Fig.9 (a) and (b), the softer subsurface in this region indicates that the rate of thermal softening is much greater than the rate of work hardening during the plastic deformation or the microstructure alteration of the subsurface [29]. In the process of the tool wear, the temperature gradually builds up, and the material softening is intensified by higher temperature, hence the surface hardness is the lowest when the number of holes drilled reaches 50. Due to the poor thermal conductivity of Ti-6Al-4V, the layer affected by temperature is small. Additionally, the white layer and the distorted layer is only about 30 μm in thickness (See Fig.10). The process of internal work hardening depends on the temperature and the mechanism of the internal stress relaxation. In helical milling process, the mechanical stress plays a major role in the subsurface. The microhardness started with a higher value, and gradually decreases to bulk hardness value (330 HV) when the depth is about 200 μm. The maximum hardness values are similar for the reported drilling processes, this is primarily due to the minor cutting edge was relatively unworn in contrast to the major cutting edge. Additionally, the minor cutting edge is in total contact with the hole wall, so the maximum hardness is not significantly affected by the wear of the major cutting edge.

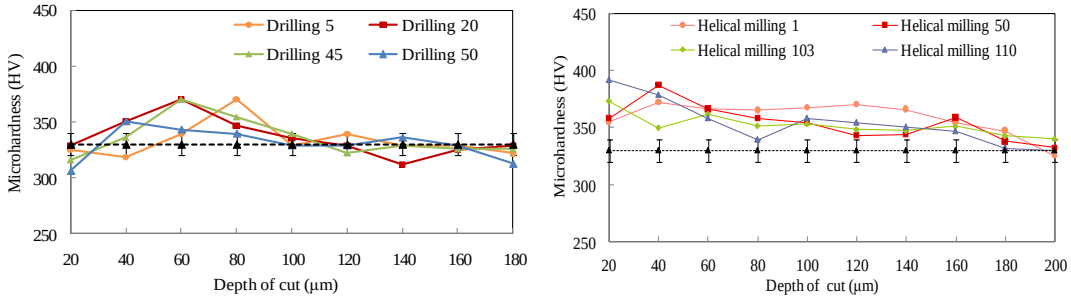

(a) (b)

Fig.9 Microhardness results: typical microhardness profiles from (a) drilling and (b) helical milling

3.3.3 Microstructure alteration

The thickness of the plastic deformation region (measured in the radial direction of the hole) was defined as the distance between the free surface of the workpiece to the depth underneath the surface where no obvious plastic deformation can be observed in the micrographs. Lower magnification optical images (×500) are used to observe the white layer and higher magnification SEM images (×3000) provide evidence for the depth of the elongated grains and their angle. As can be seen from Fig.10 (a), the maximum depth of the white layer is less than 10 μm regardless of the tools used, and the maximum depth of distorted layer and white layer is about 30 μm (See Fig.10 (b)). It is also found that the maximum depth of white layer takes place when the tool is totally broken, and the white layer is not continuous (Fig.10 (a)). This is because the increase of the contact length between the workpiece surface and the worn cutting edge produces the fracture of the white layer when the drill moves down into the workpiece. The drag of material occured down to 30 μm in the process of machining, as a result of badly worn major cutting edge and the temperature build-up.

It should also be noted that the corners of the drill are most susceptible to tool wear and have been totally fractured when hole number reaches 50. From this point more stock of material is removed by the minor cutting edge. It is likely that the minor cutting edge will have a tendency to drag the surface material rather than cut it in the cutting direction. Although the major cutting edge is not in direct contact with the machined surface, it somewhat pushes through and induces a small degree of material drag [27].

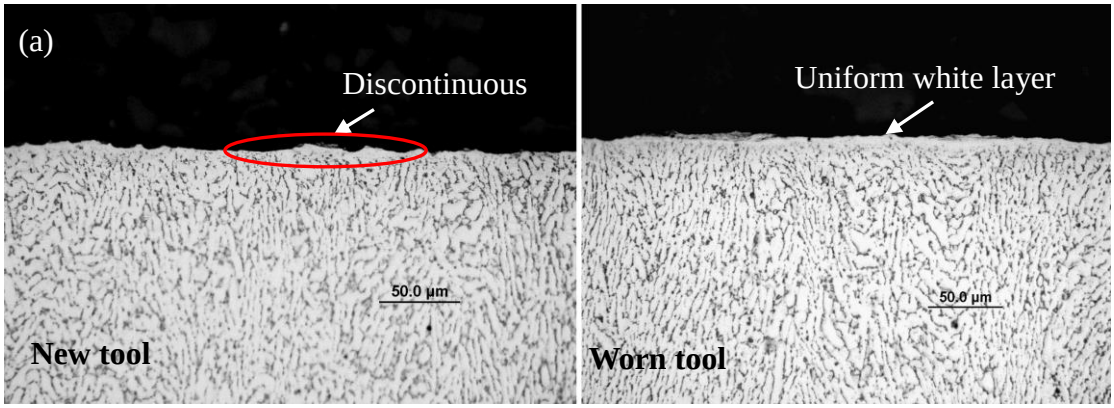

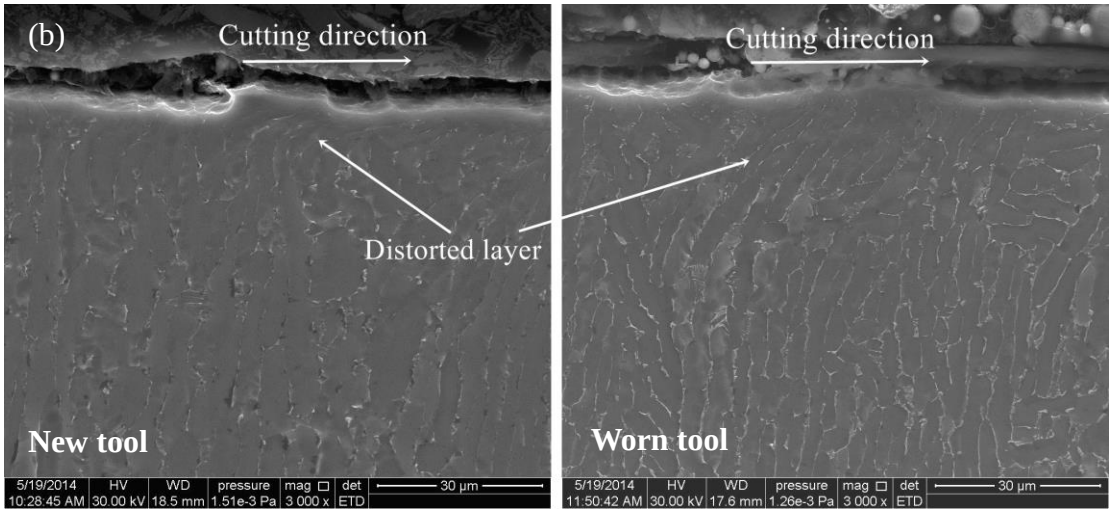

Fig.10 Microstructure of drilled surface with new and worn tool:
(a) Optical microscope and (b) SEM photography

Fig.11 show the microstructure of the hole surface in helical milling with new and worn tools. It can be clearly seen that there was no material drag occurred for the holes produced by helical milling, regardless of new or old tools used. However, a white layer can be found from Fig.11 (b), as a result of incipient melting and severe plastic deformation. In the initial stage of the tool life, there was no white layer and distorted layer observed as compared to the drilling process (See Fig.11 (a)). This is probably due to the different cutting mechanisms involved in drilling and helical milling. For the drilling process, the material on the hole wall was removed by the front cutting edge and the periphery cutting edge instead of rubbing. However, in helical milling, hole wall material is removed through an intermittent cutting process, and the periphery edge experience much lower-tangential feed per tooth. Further, the tool diameter in helical milling was smaller than that of the hole, this ensures good heat dissipation and low cutting forces. It is known that the microstructure was affected by the thermal coupling effect, therefore little change has been observed in the basic microstructure, and the white layer will only occur when the chip and the machined surface are cold welded during the helical milling process.

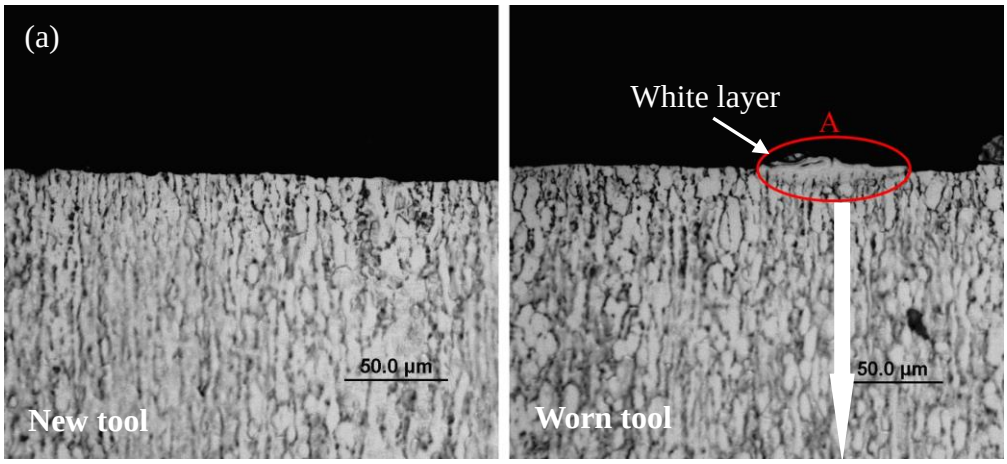

Fig.11 Microstructure of helical milled surface with new and worn tool: (a) Optical microscope and (b) SEM photography

Fig.12 shows the burr formation at steady stage of tool life for drilling and helical milling processes. It is clearly seen that the helical milling process presented a significant reduction in the burr size as compared to drilling.

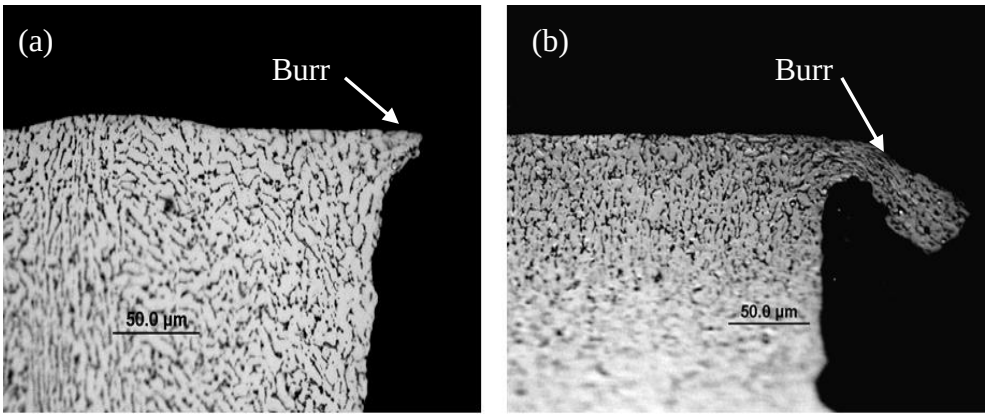

Fig.12 Exit burr formation for steady stage of tool wear (a) Helical milling (b) Drilling

3.3.4 Residual stress

Fig.13 shows the distributions of the residual stress in hole surface for drilling and helical milling processes. The underlying mechanism for the residual stress is due to the combined mechanical and thermal effects. The hole surface will exhibit tensile residual stress under high temperature, while the mechanical stress often causes a compressive residual stress. As can be seen from Fig.13, a tensile residual stress is initially generated in drilling process within the surface layer corresponding to the white layer shown in Fig.10 (a). Specifically, the maximum deformed layer depth is about 30 µm (See Fig.10), while the residual compressive stress reached the maximum value at depth of about 50 µm, and decreased gradually to zero at depth of 200 µm, which is consistent with the microhardness results.

On the other hand, compressive residual stress is generated initially for the helical milling process and reach the maximum at the hole surface. In general, the tensile residual tensile stress will reduce the fatigue life of the workpiece, while the compressive residual stress can effectively extend its fatigue life [30], therefore the helical milling can potentially improve the fatigue life of the workpiece. Compared

with Fig.10 (b), the absence of white layer and deformation layer implies that the mechanical deformation dominates in helical milling process.

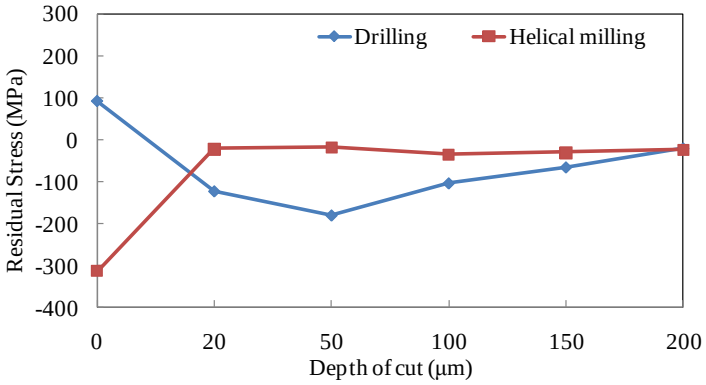

Fig.14 Residual stress of helical milling and drilling

4. Conclusion

This paper investigated the hole-making process of Ti-6Al-4V in drilling and helical milling processes. Three aspects, namely, tool wear, cutting force and the hole surface integrity (surface roughness, microhardness, microstructure and residual stress), have been considered and conclusions are as follows.

1. The tool life of helical milling cutter is much longer than that of drill cutter under the same cutting conditions in hole-making of Ti-6Al-4V. For the drilling process, tool failure was mainly due to fracture at the outer corner of the drill, and non-uniform flank wear and micro-chipping dominated the wear pattern. In contrast, crater, adhesion, chipping and flaking often occurred on the helical milling cutter.

2. The axial forces generated in both drilling and helical milling processes significantly increased with increasing tool wear, whereas the radial force only increased in helical milling but remained unchanged in drilling.

3. In the initial stage, helical milling resulted in a rougher hole surface towards the end of the milling process whereas he drilling tended to produce a smoother final finish.

4. Machined surface microhardness is a combined function of thermal softening and work hardening. The microhardness found in helical milled surface is generally higher than that of drilled surface.

5. The maximum depth of white layer was less than 10 μm in drilling process regardless of new or old tools used, and the maximum depth of distorted layer and white layer was about 30 μm. No material drag was found in the microstructure of helical milling holes, but a white layer has been found as a result of pressure welding of chips onto the workpiece surface.

6. Tensile residual stress remains in the hole produced by drilling process, while a compressive residual stress is usually produced by helical milling.

Acknowledgments

The authors are grateful for funding supports by the National Natural Science Foundation of China (51275345), Natural Science Foundation of Tianjin (11JCZDJC22800), National High Technology Research and Development Program of China (2013AA040104) and Seed Foundation of Tianjin University.

Reference

[1] Sharif, S., Rahim, E.A., Performance of coated-and uncoated-carbide tools when drilling titanium alloy —Ti6Al4V. *J. Mat. Proc. Tech.*, 2007, Vol. 185, pp. 72-76.

[2] Machado, A.R., Wallbank J., Machining of titanium and its alloys—a review, *Proc. Inst. Mech. Eng*, 1990, Vol. 204, pp. 53–60.

[3] Wang, Z.G., Wong, Y.S., Rahman M., High-speed Milling of Titanium Alloys using Binderless CBN Tools, *Int. J. Mach. Tools Manuf.*, 2005, Vol. 45, pp. 105-114.

[4] Wang, Z.G., Rahman, M., Wong, Y.S., Tool Wear Characteristics of Binderless CBN Tools Used in High-Speed Milling of Titanium Alloys, *Wear*, 2005, Vol. 258, pp. 752-758.

[5] Li, L., Chang, H., Wang, M., et al. Temperature Measurement in High Speed Milling, *Key Eng. Mat.*, 2004, Vol. 259, pp. 804-808.

[6] Rossman, E.F., Collected Thoughts on High Speed Machining of Titanium, *SME Tech. Paper*, 2003, MR03-347, pp. 1-8.

[7] Narutaki, N., Murakoshi, A., Study on machining of titanium alloys, *CIRP Ann*, 1983, Vol. 32, pp. 65 – 69.

[8] Hartung, P.D., Kramer, B.M., Tool wear in machining titanium, *CIRP Ann*, 1982, Vol. 31, pp. 75–80.

[9] Schroeder, P.T., Widening interest in twist drill, *Modern Mach. Shop*, 1998, Vol. 71, pp. 106–113.

[10] Sharif, S., Venkatesh, V.C., Rahim, E.A., The Effects of Coatings on the Performance of Carbide Tools when Drilling Titanium Alloy Ti-6Al-4V, *8thCIRP Int. Work*, 2005, pp. 577-581.

[11] Zeilmann, R.P., Weingaertner, W.L., Analysis of Temperature during Drilling of Ti6Al4V with Minimal Quantity of Lubricant, *J. Mat. Proc. Tech.*, 2006, Vol. 179, pp. 124-127.

[12] Cantero, J.L., Tardio, M.M., Canteli, J.A., et al. Dry Drilling of Alloy Ti-6Al-4V, *Int. J. Mach. Tools Manuf.*, 2005, Vol. 45, pp. 1246-1255.

[13] Che-Haron, C.H., Tool life and surface integrity in turning titanium alloy, *J. Mat. Proc. Tech.*, 2001, Vol. 118, pp. 231-237.

[14] Che-Haron, C.H., Jawaid, A., The effect of machining on surface integrity of titanium alloy Ti-6%Al-4%V. *J. Mat. Proc. Tech.*, 2005, Vol. 166, pp. 188-192.

[15] Sharman, A.R.C, Amarasinghe, A., Ridgway K., Tool life and surface integrity aspects when drilling and hole-making in Inconel 718, *J. Mat. Proc. Tech.*, 2008, Vol. 200, pp. 424-432.

[16] Erween, A.R., Safian, S., Investigation on tool life and surface integrity when drilling Ti -6Al-4V and Ti -5Al-4V-Mo/Fe, *JSME International Journal*, 2006, Vol. 49, pp. 340-345.

[17] Iyer, R., Koshy, P., Ng, E., Helical milling: an enabling technology for hard machining precision holes in AISI D2 tool steel. *Int. J. Mach. Tools Manuf.*, 2007, Vol. 47, pp. 205-210

[18] Sasahara, H., Kawasaki, M., Tsutsumi, M., Helical feed milling with MQL for boring of aluminum alloy. *J. adv. Mech. Des., syst., manuf.*, 2008, Vol. 2, pp. 1030-1040.

[19] Brinksmeier, E., Fangmann, S., Meyer, I., Orbital drilling kinematics. *Prod. Eng. Res. Devel.*, 2008, Vol. 2, pp. 277-283.

[20] Li, Zh.Q., Liu, Q., Surface topography and roughness in hole-making by helical milling. *Int. J. Adv. Manuf. Technol.*, 2013, Vol. 6, pp. 1415-1425.

[21] Liu, Ch.Y., Wang, G., Dargusch, M.S., Modeling, simulation and experimental investigation of cutting forces during helical milling operations, *Int. J. Adv. Manuf. Technol.*, 2012, Vol. 63, pp. 839-850.

[22] Sadek, A., Meshreki, M., Attia, M.H., Characterization and optimization of orbital drilling of woven carbon fiber reinforced epoxy laminates, *CIRP Annals – Manuf. Technol.*, 2012, Vol. 61, pp. 123-126.

[23] Denkena, B., Boehnke, D., Dege, J.H., Helical milling of CFRP-titanium layer compounds. *CIRP J. Manuf. Sci. Technol.*, 2008, Vol. 1, pp. 64-69.

[24] Moussaoui, K., Mousseigne, M., Johanna, S., et al. Influence of milling on surface integrity of Ti6Al4V—study of the metallurgical characteristics: microstructure and microhardness. *Int. J. Adv. Manuf. Technol.*, 2013, Vol. 67, pp. 1477–1489.

[25] Li, H., He, G.Y., Qin, X.D., et al. Tool wear and hole quality investigation in dry helical milling of Ti-6Al-4V alloy, *Int. J. Adv. Manuf. Technol.*, 2014, Vol. 71, pp. 1511-1523.

[26] Daymi, A., et al, Surface integrity in high speed end milling of titanium alloy Ti-6Al-4V. *Mat. Sci. Tech.*, 2011, Vol. 27, pp. 387-394.

[27] Herbert, C.R.J., Kwong J., et al. An evaluation of the evolution of workpiece surface integrity in hole-making operations for a nickel-based superalloy. *J. Mat. Proc. Tech.*, 2012, Vol. 212, pp. 1723-1730.

[28] Kwong, J., Axinte, D.A., et al. Minor cutting edge -workpiece interactions in drilling of an advanced nickel-based superalloy. *Int. J. Mach. Tools Manuf.*, 2009, Vol. 49, pp. 645-658.

[29] Liu, J., Ren, C.Z., Qin, X.D., et al. Prediction of heat transfer process in helical milling, *Int. J. Adv. Manuf. Technol.*, 2014, Vol. 72, pp. 693-705.

[30]Ginting, A., Nouari, M., Surface integrity of dry machined titanium alloys. *Int. J. Mach. Tools Manuf.*, 2009, Vol. 49, pp. 325-332.
[31]Yao, C.F., Tan, L., Ren, J.X., et al. Surface Integrity and Fatigue Behavior for High-Speed Milling Ti-10V-2Fe-3Al Titanium Alloy. *J. Fail. Anal. & Prev.*, 2014, Vol.14, pp.102-112.